UDK 620.18:66.021.3.081.3:547.556
Original scientific article/Izvirni znanstveni članek

ISSN 1580-2949
MTAEC9, 54(4)529(2020)

ADSORPTION BEHAVIOR OF POLYANILINE MICRO/NANOSTRUCTURES FOR METHYL ORANGE

ADSORPCIJA POLIANILNIH MIKRO- IN NANOSTRUKTUR ZA METILORANŽ

Cuijuan Xing, Aiqing Xia, Ling Yu, Yongchao Hao, Lili Dong, Zhiju Zhao, Guiquan Guo*, Yu Wang, Limin Tian, Mengze Sun

School of Chemistry and Chemical Engineering, Xingtai University, No. 88 Quanbei East Street, Qiaodong District, Xingtai 054001, China

Prejem rokopisa – received: 2019-11-06; sprejem za objavo – accepted for publication: 2020-03-01

doi:10.17222/mit. 2019.270

Polyaniline (PANI) nanofibers were successfully synthesized with ammonium persulfate as an oxidant. The adsorption behavior of methyl orange (MO) on PANI at different parameters was investigated. Equilibrium studies demonstrated the use of the Langmuir adsorption model and the maximum adsorption capacity (Q_e) was calculated to be 315.3 mg·g^{-1} at 313 K. A kinetic study revealed that the MO adsorption on PANI followed the pseudo-second-order kinetic model. Experimental results suggest that PANI nanofibers have the potential to be used as low-cost and efficient adsorbent materials for the removal of organic pollutants from water.

Keywords: PANI micro/nanostructures, sorption, methyl orange (MO)

Avtorji tega prispevka opisujejo uspešno sintezo polianilnih (PANI) nanovlaken s pomočjo uporabe amonijevega persulfata kot oksidanta. Raziskovali so obnašanje metiloranža (MO) med adsorpcijo na polianilnih nanovlaknih pri različnih parametrih. Ravnotežne študije so pri uporabi Langmuirjevega adsorpcijskega modela dale vrednost maksimalne adsorpcijske kapacitete (Q_e) 315,3 mg·g^{-1} pri 313 K. Kinetične študije pa so pokazale, da adsorpcija metiloranža na polianilnih vlaknih sledi pseudokinetičnemu modelu drugega reda. Eksperimentalni rezultati kažejo, da bi bila polianilna nanovlakna lahko uporabna kot učinkovit nizko cenovni adsorpcijski material (adsorbent) za odstranitev organskih nečistoč iz vode.

Ključne besede: polianilne mikro- in nanostrukture, sorpcija, metiloranž

1 INTRODUCTION

Due to the indiscriminate disposal of organic pollutants, water pollution has been a rising worldwide environmental concern.[1–2] In particular, dyes, which are the main organic contaminants from the dye manufacturing and textile branches, are necessary to be removed from the waste water.[3] The removal of organic dyes from natural water resources does not only protect the environment itself, but also stops the toxic-dye transfer within food chains. Traditional techniques for treating organic dyes include membrane filtration, ion exchange, precipitation, adsorption and coagulation.[4–6] However, it is noteworthy to mention that adsorption is the most widely used method because of its ease of operation and relatively low cost.[7] Several adsorbents were studied for dye removal including hybrid xerogel, caly, activated carbon, sepiolite and pansil.[8–10] The development of adsorbents with a high adsorption capacity and effectivity is attracting attention of scientists.

Amino groups, one of the most effective chelating functional groups, have attracted special attention with regard to the enrichment of various contaminants from aqueous solutions due to their high nucleophilicity and reactivity.[11] Polyaniline (PANI), a well-known conducting polymer, has received a great deal of interest due to its simple preparation, controllable electrical conductivity, environmental stability, good redox reversibility and low cost. Recently, PANI and its composites have been used effectively for the removal of inorganic and organic pollutants. They possess a large amount of amine and imine groups, which can interact with heavy metals and organic pollutants, making them suitable for pollutant adsorption from aqueous solutions. Previous studies suggested that PANI composites are promising adsorbents for Cr (IV),[12–14] Hg (II),[15] Pb (II)[16] and tannic acid.[17] PANI exhibits a high adsorption capacity for tannic acid. Wan observed a significant improvement in the humic-acid adsorption capacity when PANI was encapsulated on the surface of ATP.[18] An enhanced HA adsorption was associated with electrostatic interactions between the amine and imine groups of the adsorbents and HA molecules in the solution.

Based on the premise that nitrogen atoms in PANI can interact with organic pollutants in an aqueous solution, PANI is expected to be an efficient and economic adsorbent for removing dyes. Herein, PANI was synthesized with a chemical oxidation to remove MO from an aqueous solution. By employing batch experiments, the removal of MO on PANI was investigated

*Corresponding author's e-mail:
guoguiquan1979@163.com (Guiquan Guo)

across a range of solution-chemistry conditions, including time, temperature and ionic strength. The adsorption kinetics and isotherms were investigated for a possible mechanism. This study provides new insights into the MO removal from aqueous solutions using PANI, which can broaden the applicability of PANI to wastewater cleanup.

2 EXPERIMENTAL PART

2.1 Materials

Aniline monomer (ANI, Beijing Chem. Co.) was distilled under vacuum. Ammonium persulfate (APS), methyl orange (MO) and other reagents were purchased from Beijing Chem. Co. and used without further purification.

2.2 Polymerization

Polyaniline was prepared by polymerizing ANI at room temperature in an aqueous solution. Briefly, ANI (10 mmol) was dissolved in 25 mL of distilled water with supersonic stirring. Then an aqueous solution of APS (2.3 g, 10 mmol), dissolved in 25 mL of distilled water was dropped into the above solution and vigorously stirred at room temperature. After having been stirred for about 12 h, the product was collected with vacuum filtration, and then washed with water, ethanol and ether several times, respectively. Finally, the product was being dried under vacuum at room temperature for 24 h.

2.3 Characterization

The morphology of the PANI was characterized with field-emission scanning electron microscopy (FESEM, JSM-6700F). FTIR and UV-Vis spectroscopy were carried out to study the molecular structures. The FTIR spectra of PANI in KBr pellets were recorded using an IFS-113 V instrument. The resolution of the measurements and the number of scans were 4 cm^{-1} and 16, respectively. UV-Vis spectroscopy of PANI in *m*-cresol was measured with a Hitachi UV3100. The crystal structures of the resulting polymer were characterized with X-ray diffraction (a Micscience Model M18XHF diffractometer). The concentration of MO in the solution was analyzed using a UV-Vis spectrum instrument (UV-2200, Beijing Beifen-Ruili Analytical Instrument CO., Ltd).

2.4 Sorption experiments

2.4.1 Kinetic-sorption experiments

The sorption experiments were performed using a batch technique. Briefly, samples of 0.1000±0.0001 g of PANI were added into a series of 100 mL MO solution at 298 K in a temperature-controlled shaker (SHY-2A, Danyang Appliance Co., Jiangsu). The agitation speed was 150 min^{-1}. The samples were withdrawn at appropriate time intervals. Then the mixture was filtered through a 0.2-μm pore membrane. The supernatant of each sample was analyzed using UV spectrometry based on the law of Lambert-Beer, identified as the equilibrium concentration of MO. The MO adsorbed on a PANI sample was calculated from the difference between the initial and equilibrium MO concentrations. These experiments were carried out under the same conditions at three levels, and the relative error was <5 %. The adsorption capacity (Q_e $mg \cdot g^{-1}$) of the MO adsorbed onto PANI was obtained from Equation (1) and used for a further adsorption-isotherm analysis:

$$Q_e = \frac{(C_0 - C_e)V}{m} \quad (1)$$

where C_0 and C_e are the initial and equilibrium concentrations of MO. V is the volume of the MO solution (L) and m is the weight of the PANI adsorbent (g).

2.4.2 Equilibrium sorption experiments

A batch method was also used to obtain sorption isotherms. Isotherm experiments were conducted in distilled water with various initial concentrations of MO

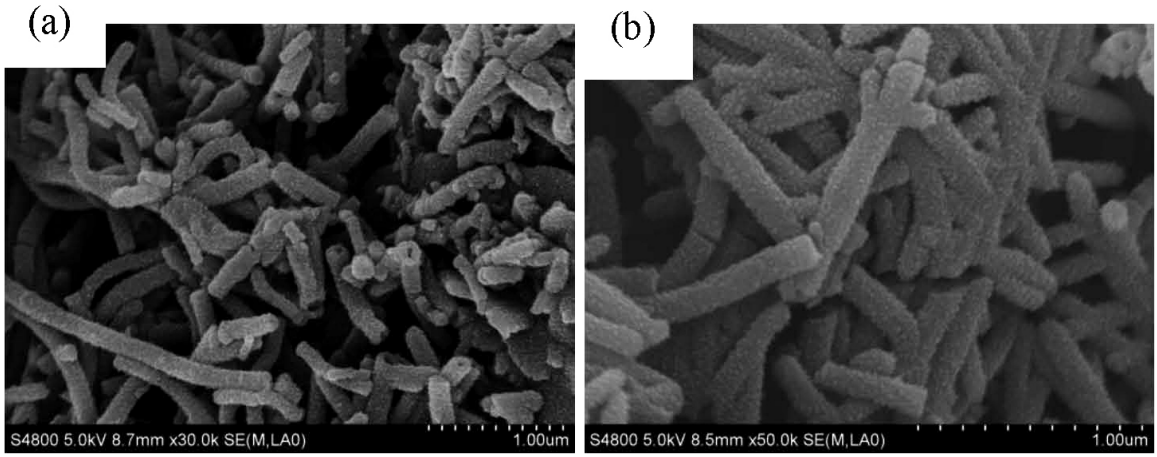

Figure 1: SEM images of PANI micro/nanostructures

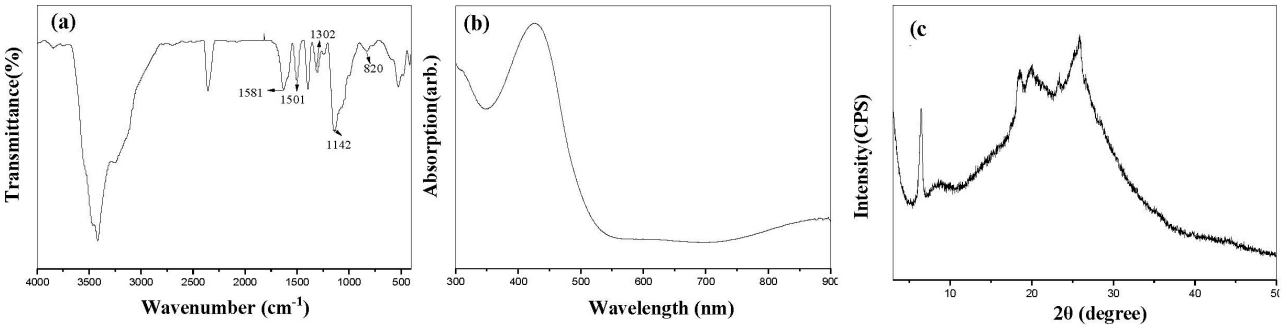

Figure 2: a) FTIR spectra, b) UV-vis absorptionand c) XRD patterns of PANI micro/nanostructures

(5-250 mg·dm^{-1}). An amount of 0.1000±0.0001 g of PANI was added to 250-mL glass-stoppered flasks. Each flask contained 100 mL of solution. The flasks were then agitated at a constant speed of 150 min^{-1} in a temperature-controlled shaker. After equilibrium was established, the supernatants were separated. The residual MO concentrations were analyzed and the amount of sorption onto PANI was determined as in the kinetic experiments.

3 RESULTS AND DISCUSSION

3.1 Surface morphology of the PANI products

Scanning-electron-microscopy (SEM) images of PANI are shown in **Figure 1**. It can be seen from the figure that nanofibers with an average diameter of 220 nm were obtained. There are protuberances on the surfaces of nanofibers, providing a good platform for the MO adsorption.

3.2 Structural and chemical characterization of the PANI products

FTIR and UV-vis spectroscopy were used to characterize the molecular structure of PANI. Typical FTIR spectra (**Figure 2a**) showed that the characteristic absorption bands for the PANI fibers are similar to those of PANI.[19] For example, the C=C stretching deformation of the quinoid (1581 cm^{-1}) and benzenoid rings (1501 cm^{-1}), the C-N stretching of the secondary aromatic amine (1302 cm^{-1}), the aromatic C-H in-plane bending (1142 cm^{-1}), and the out-of-plane deformation of C-H in the 1,4-disubstituted benzene ring (820 cm^{-1}) are observed. The UV-vis absorbance spectra of the PANI sample dissolved in *m*-cresol is shown in **Figure 2b**. Bands at 430 nm and >800 nm were observed for PANI, and they were assigned to polaron bands of the emeraldine salt of PANI.[20] The band at 430 nm corresponds to the partially oxidized form of PANI, most likely in the intermediate state between the leucoemeraldine form containing benzenoid rings and the emeraldine form containing conjugated quinoid rings in the main polymer chain. The emeraldine form transformed into the fully oxidized pernigraniline form, characterized by a wide band at around 800 nm.

Figure 2c shows XRD patterns for PANI. PANI exhibits a broad featureless XRD pattern centered around 2θ = 20–30°, indicating that the sample is probably amorphous. Some additional sharp peaks centered at 2θ = 6.5°, 18.5°, 20.4° and 25.5° are observed and can be attributed to the periodicity perpendicular and parallel to the polymer chain, respectively.[21]

3.3 Adsorption performance of PANI

3.3.1 Sorption kinetics

In order to determine the MO sorption equilibration time and investigate the kinetic characteristics of the sorption, experiments were carried out with there initial MO concentrations of 100 mg·L^{-1}, 200 mg·L^{-1} and 250 mg·L^{-1}. **Figure 3** shows the plots of Q_t-t at 298 K. The results indicate that adsorption equilibrium was reached within 120 min as the initial MO concentration is 100 mg·L^{-1}. As a comparison, the initial MO concentration increased to 200 mg·L^{-1} and 250 mg·L^{-1}, while the adsorption time before reaching the equilibrium state was 300 min. The sorption equilibration time was therefore determined to be 360 min to ensure a complete equilibration.

Pseudo-second-order Equation (2) was tried to interpret the kinetic curves and it can be expressed as:

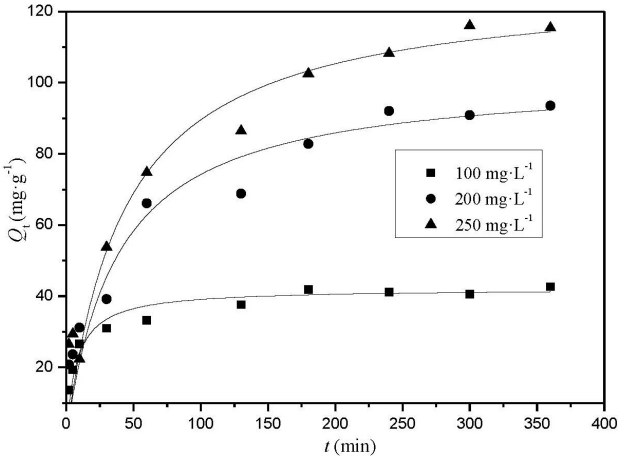

Figure 3: Sorption-kinetic curves of MO on the PANI micro/nanostructure (line: pseudo-second-order model fitting)

$$\frac{dQ_t}{dt} = k_2 (Q_e - Q_t)^2 \quad (2)$$

where Q_e and Q_t (mg·g^{-1}) are the sorption amounts of the sorbate at equilibrium and various times t (min), while k_2 (g·mg^{-1}·min^{-1}) is the rate constant.

Sorption parameters were obtained by fitting the experimental data using a non-linear regression method, as shown in **Table 1**. In the pseudo-second-order kinetics, the calculated Q_e values were nearly the same as the experimental values. Based on the correlation coefficients, r^2, the pseudo-second-order equation describes the curves well.

Table 1: Kinetic parameters of the pseudo-second-order models for MO sorption on PANI micro/nanostructures at different initial concentrations (298 K)

C_0/mg·dm^{-1}	Q_e(cal)/mg·g^{-1}	k_2/g·mg^{-1}·min^{-1}	r^2
100	42.10	0.003090	0.9227
200	102.0	0.0002619	0.9175
250	127.9	0.0001828	0.9375

3.3.2 Sorption isotherms

It is well established that temperature is an important factor influencing any adsorption process. **Figure 4** shows the adsorption isotherms of MO at four temperatures (293, 298, 303 and 313) K. The experimental data for MO on PANI are analyzed using the Langmuir adsorption isotherm model, which is applicable to highly heterogeneous surfaces. Equation (3) is given as:

$$Q_e = \frac{Q_m K_L C_e}{1 + K_L C_e} \quad (3)$$

where Q_e is the adsorption amount of MO on the adsorbent (mg·g^{-1}) at an equilibrium state, Q_m is the adsorption capacity of MO on the adsorbent (mg·g^{-1}), C_e is the equilibrium concentration of MO (mg·L^{-1}), and K_L is the Langmuir adsorption constant, related to the adsorption energy. It can be seen from **Table 2** that the Langmuir model shows good agreement with the experimental data. As the temperature increases, MO molecules are more favorably adsorbed on PANI. The adsorption capacity of MO is 131.1 mg·g^{-1} and 139.9 mg·g^{-1} at 293 K and 298 K. As the temperature increases to 303 K and 313 K, the adsorption capacity of MO increases to 157.6 mg·g^{-1}and 315.3 mg·g^{-1}, respectively. A temperature increase is known to increase the rate of diffusion of adsorbate molecules across the external boundary layer and in the internal pores of the adsorbent.

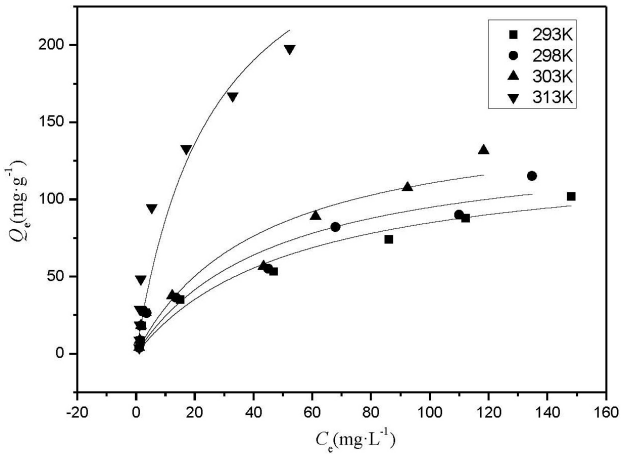

Figure 4: Adsorption isotherms of MO on PANI micro/nanostructures at different temperatures

Table 2: Langmuir constants for the adsorption of MO onto PANI micro/nanostructures at different temperatures

T/K	Q_m/mg·g^{-1}	K_L/L·mg^{-1}	r^2
293	131.1	0.01834	0.9124
298	139.9	0.02101	0.9218
303	157.6	0.02338	0.9302
313	315.3	0.03800	0.9252

3.3.3 Thermodynamic parameters

Thermodynamic parameters of the MO sorption were evaluated, including the standard free-energy change (ΔG^θ), standard enthalpy change (ΔH^θ) and standard entropy change (ΔS^θ), which is important for understanding the sorption process. The parameters were calculated using Equations (4) and (5):

$$\Delta G^\theta = -RT \ln K \quad (4)$$

$$\ln K = -\frac{\Delta H^\theta}{RT} + \frac{\Delta S^\theta}{R} \quad (5)$$

R is the universal gas constant and T is the Kelvin temperature; K is the thermodynamic equilibrium constant for the adsorption process. In our study, we used the constant derived from the Langmuir model (K_L). The values of ΔH^θ and ΔS^θ were obtained from the plots of ln K versus 1/T. The values of these thermodynamic parameters are listed in **Table 3**.

The positive value of ΔH^θ suggests that the sorption was an endothermic process, indicating that a higher temperature is beneficial to the sorption process. The positive value of ΔS^θ demonstrates increased randomness at the solid-solution interface during the adsorption of MO on PANI, indicating a strong tendency toward the MO adsorption. The free-energy ΔG^θ values were negative over the entire temperature range, indicating that the MO adsorption onto PANI was thermodynamically feasible and could occur spontaneously.

Table 3: Thermodynamic parameters for MO adsorption onto PANI micro/nanostructures

T/K	$K_L \times 10^{-6}$/ mL·g^{-1}	ΔG^θ/ kJ·mol^{-1}	ΔH^θ/ kJ·mol^{-1}	ΔS^θ/ J·mol^{-1}·K^{-1}
293	0.01834	–23.91	27.00	58.61
298	0.02101	–24.61		
303	0.02338	–25.34		
313	0.03800	–27.44		

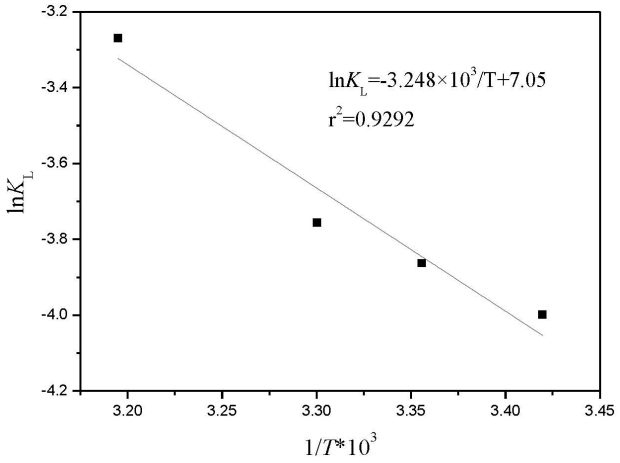

Figure 5: Van't Hoff plot for the MO sorption onto PANI micro/nanostructures

The sorption isotherms of MO in NaCl solutions, having concentrations of 0 mol·L^{-1}, 0.5 mol·L^{-1} and 1.0 mol·L^{-1} were investigated in our study. As shown in **Figure 6**, sorption isotherms of MO on PANI accorded well with the Langmuir model. The constants of the Langmuir sorption equation and the correlation coefficients are listed in **Table 4**. This table shows that the Q_m values increased from 139.9 mg·g^{-1} to 210.8 mg·g^{-1} when the concentration of NaCl increased from 0 to 0.5 mol·L^{-1}. While the concentration of NaCl increased to 1.0 mol·L^{-1}, the Q_m values decreased to 181.0 mg·g^{-1}. These results conclusively demonstrate that NaCl had a strong influence on the sorption capacity of PANI. The reasons can be explained with two aspects. Firstly, for hydrophobic organic chemicals such as MO, its water solubility plays an important role in the sorption behavior.[22] A solution of NaCl contains inorganic ionic species of Na^+ and Cl^-, which can push organic compounds to the surface of the adsorbent, hence reducing the water solubility of organic compounds. The reason for this is attributed to "salting out". Meanwhile, the

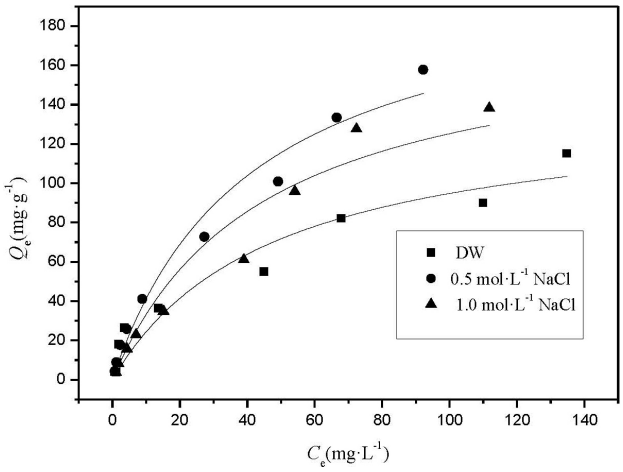

Figure 6: Adsorption isotherms of MO on PANI micro/nanostructures in different media

inorganic ionic species of Na^+ and Cl^- make the ionization equilibrium of the MO adsorbed to PANI. On the other hand, the Na^+ and Cl^- in a solution can increase the doping level and decease efficient activity sites. Therefore, it is reasonable to expect that a higher concentration of NaCl (1.0 mol·L^{-1}) might go against the adsorption of MO on PANI.

Table 4: Langmuir constants for the adsorption of MO onto PANI micro/nanostructures in the presence of various concentrations of NaCl

C_{NaCl}/mol·dm^{-1}	Q_m/mg·g^{-1}	K_L/L·mg^{-1}	r^2
0	139.9	0.02101	0.9218
0.5	210.8	0.02425	0.9779
1.0	181.0	0.02243	0.9534

4 CONCLUSIONS

In this study, PANI was successfully prepared via a facile-solution route, using ammonium peroxydisulfate as the initiator. The sorption of MO on PANI under various conditions was investigated to evaluate its kinetic and thermodynamic behavior. The results obtained are as follows:

1) The sorption equilibrium was achieved within 5 h. The kinetics of the process can be described with a pseudo-second-order kinetic-rate equation. The initial concentration of MO influenced the sorption rate. With an increase in the initial concentration from 100 mg·L^{-1} to 250 mg·L^{-1}, the rate constant decreased from 3.890 ×10^{-3} to 3.125×10^{-4} g·mg^{-1}·min^{-1}.
2) Sorption isotherms of MO on PANI can be described well with the Langmuir equation. Thermodynamic parameters of the sorption were determined. ΔG^{θ} (298 K) was found to be 24.61 kJ·mol^{-1}. This value indicated that the process was spontaneous. ΔH^{θ} and ΔS^{θ} were 27.00 kJ·mol^{-1} and 58.61 J·mol^{-1}·K^{-1}. Electrostatic interactions between positively charged polymer chains and anionic dye were responsible for the high adsorption capacity for MO.
3) The NaCl concentration and the temperature affected the sorption behavior. A higher sorption capacity was found for a higher temperature. With an increase in the NaCl concentration from 0 to 0.5 mol·L^{-1}, the Q_m increased from 139.9 mg·g^{-1} to 210.8 mg·g^{-1}. However, the Q_m decreased to 181.0 mg·g^{-1} when the concentration of NaCl increased to 1.0 mol·L^{-1}.

Acknowledgments

We acknowledge the support of the National Science Foundation for Young Scientists of the Hebei Province (Grant Nos. E2018108011 and B2017108031) and Municipal People's Livelihood Science and Technology Security Special Project of the Xingtai City in 2018 (2018ZZ18).

5 REFERENCES

[1] B. Meunier, Chemistry: catalytic degradation of chlorinated phenols, Science, 296 (**2002**) 5566, 270–271, doi:10.1126/science.1070976

[2] W. Ma, J. Li, X. Tao, J. He, Y. Xu, J. Yu, J. Zhao, Efficient degradation of organic pollutants by using dioxygen activated by resin-exchanged iron(II) bipyridine under visible irradiation, Angew. Chem. Int. Ed., 42 (**2003**) 9, 1029–1031, doi:10.1002/anie.200390264

[3] M. T. Yagub, T. K. Sen, S. Afroze, N. M. Ang, Dye and its removal from aqueous solution by adsorption: a review, Adv. Colloid Interface Sci., 209 (**2014**) 172–184, doi:10.1016/j.cis.2014.04.002

[4] S. Wang, Z. H. Zhu, Characterisation and environmental application of an Australian natural zeolite for basic dye removal from aqueous solution, J. Hazard. Mater., 136 (**2006**) 3, 946–952, doi:10.1016/j.jhazmat.2006.01.038

[5] A. Meng, J. Xing, Z. Li, Q. Li, Cr-doped ZnO nanoparticles: synthesis, characterization, adsorption property, and recyclability, ACS Appl. Mater. Interfaces, 7 (**2015**) 49, 27449–27457, doi:10.1021/acsami.5b09366

[6] D. Mahanta, G. Madras, S. Radhakrishnan, S. Patil, Adsorption of sulfonated dyes by polyaniline emeraldine salt and its kinetics, J. Phys. Chem. B, 112 (**2008**) 33, 10153–10157, doi:10.1021/jp803903x

[7] V. K. Gupta, A. Mittal, V. Gajbe, J. Mittal, Adsorption of basic fuchsin using waste materials-bottom ash and deoiled soya-as adsorbents, J. Colloid Interface Sci., 319 (**2008**) 1, 30–39, doi:10.1016/j.jcis.2007.09.091

[8] Z. Wu, H. Joo, K. Lee, Kinetics and thermodynamics of the organic dye adsorption on the mesoporous hybrid xerogel, Chem. Eng. J., 112 (**2005**) 1–3, 227–236, doi:10.1016/j.cej.2005.07.011

[9] B. H. Stefan, W. W. Kenneth, P. S. Pene, Specific adsorption of nitroaromatic explosives and pesticides to clay minerals, Environ. Sci. Technol., 30 (**1996**) 2, 612–622, doi:10.1021/es9503701

[10] Y. C. Sharma, A. S. K. Sinha, S. N. Upadhyay, Characterization and adsorption studies of cocos nucifera L. activated carbon for the removal of methylene blue from aqueous solutions, J. Chem. Eng. Data, 55 (**2010**) 8, 2662–2667, doi:10.1021/je900937f

[11] J. M. González-Domínguez, M. González, A. Ansón-Casaos, A. M. Di´ez-Pascual, Effect of various aminated single-walled carbon nanotubes on the epoxy cross-linking reactions, J. Phys. Chem. C, 115 (**2011**) 15, 7238–7248, doi:10.1021/jp110830y

[12] A. E. Chávez-Guajardo, J. C. Medina-Llamas, L. Maqueira, C. A. S. Andrade, K. G. B. Alves, C. P. Melo, Efficient removal of Cr (VI) and Cu (II) ions from aqueous media by use of polypyrrole/maghemite and polyaniline/maghemite magnetic nanocomposites, Chem. Eng. J., 281 (**2015**), 826–836, doi:10.1016/j.cej.2015.07.008

[13] X. Y. Han, L. G. Gai, H. H. Jiang, L. C. Zhao, H. Liu, W. Zhang, Core–shell structured Fe_3O_4/PANI microspheres and their Cr(VI) ion removal properties, Synthetic Met., 171 (**2013**) 1–6, doi:10.1016/j.synthmet.2013.02.025

[14] Q. Li, L. Sun, Y. Zhang, Y. Qian, J. P. Zhai, Characteristics of equilibrium, kinetics studies for adsorption of Hg(II) and Cr(VI) by polyaniline/humic acid composite, Desalination, 266 (**2011**) 1, 188–194, doi:10.1016/j.desal.2010.08.025

[15] H. Cui, Y. Qian, Q. Li, Q. Zhang, J. P. Zhai, Adsorption of aqueous Hg(II) by a polyaniline/attapulgite composite, Chem. Eng. J., 211–212 (**2012**), 216–223, doi:10.1016/j.cej.2012.09.057

[16] Y. F. Yang, W. J. Wang, M. Li, H. F. Wang, Preparation of PANI grafted at the edge of graphene oxide sheets and its adsorption of Pb(II) and methylene blue, Polym. Composite, 39 (**2016**) 5, 1663–1673, doi:10.1002/pc.24114

[17] C. C. Sun, B. W. Xiong, Y. Pan, H. Cui, Adsorption removal of tannic acid from aqueous solution by polyaniline: Analysis of operating parameters and mechanism, J. Colloid Interface Sci., 487 (**2017**), 175–181, doi:10.1016/j.jcis.2016.10.035

[18] T. Wen, Q. H. Fan, X. L. Tan, Y. T. Chen, C. L. Chen, A. W. Xu, Q. H. Fan, A core–shell structure of polyaniline coated protonic titanate nanobelt composites for both Cr(VI) and humic acid removal, Polym. Chem., 7 (**2016**) 4, 785–794, doi:10.1039/C5PY01721A

[19] Z. M. Zhang, J. Y. Deng, J. Y. Shen, M. X. Wan, Z. J. Chen, Chemical one step method to prepare polyaniline nanofibers with electromagnetic function, Macromol. Rapid. Comm., 28 (**2007**) 5, 585–590, doi:10.1002/marc.200600729

[20] Y. Cao, P. Smith, A. J. Heeger, Spectroscopic studies of polyaniline in solution and in spin-cast films, Synthetic Met., 32 (**1989**), 263–281

[21] J. P. Pouget, M. E. Jozefowice, A. J. Epstein, X. M. Tang, A. G. MacDiarmid, X-ray structure of polyaniline, Macromolecules, 24 (**1991**) 3, 779–789, doi:10.1021/ma00003a022

[22] X. K. Zhao, G. P. Yang, P. Wu, N. H. Li, Study on adsorption of chlorobenzene on marine sediment, J. Colloid Interf. Sci., 243 (**2001**) 2, 273–279, doi:10.1006/jcis.2001.7859